RESEARCH ARTICLE

Highly Accelerated Compressed-Sensing 4D Flow for Intracardiac Flow Assessment

Akos Varga-Szemes, MD, PhD,[1] Moritz Halfmann, MD,[2,3] U. Joseph Schoepf, MD,[1] Ning Jin, PhD,[4] Anton Kilburg,[2] Danielle M. Dargis, BS,[1] Christoph Düber, MD,[2] Amir Ese, MD,[2] Gilberto Aquino, MD,[1] Fei Xiong, MS,[4] Karl-Friedrich Kreitner, MD,[2] Michael Markl, PhD,[5,6] and Tilman Emrich, MD[1,2,3*]

Background: Four-dimensional (4D) flow MRI allows for the quantification of complex flow patterns; however, its clinical use is limited by its inherently long acquisition time. Compressed sensing (CS) is an acceleration technique that provides substantial reduction in acquisition time.
Purpose: To compare intracardiac flow measurements between conventional and CS-based highly accelerated 4D flow acquisitions.
Study Type: Prospective.
Subjects: Fifty healthy volunteers (28.0 ± 7.1 years, 24 males).
Field Strength/Sequence: Whole heart time-resolved 3D gradient echo with three-directional velocity encoding (4D flow) with conventional parallel imaging (factor 3) as well as CS (factor 7.7) acceleration at 3 T.
Assessment: 4D flow MRI data were postprocessed by applying a valve tracking algorithm. Acquisition times, flow volumes (mL/cycle) and diastolic function parameters (ratio of early to late diastolic left ventricular peak velocities [E/A] and ratio of early mitral inflow velocity to mitral annular early diastolic velocity [E/e′]) were quantified by two readers.
Statistical Tests: Paired-samples *t*-test and Wilcoxon rank sum test to compare measurements. Pearson correlation coefficient (*r*), Bland–Altman-analysis (BA) and intraclass correlation coefficient (ICC) to evaluate agreement between techniques and readers. A *P* value < 0.05 was considered statistically significant.
Results: A significant improvement in acquisition time was observed using CS vs. conventional accelerated acquisition (6.7 ± 1.3 vs. 12.0 ± 1.3 min). Net forward flow measurements for all valves showed good correlation ($r > 0.81$) and agreement (ICCs > 0.89) between conventional and CS acceleration, with 3.3%–8.3% underestimation by the CS technique. Evaluation of diastolic function showed 3.2%–17.6% error: E/A 2.2 [1.9–2.4] (conventional) vs. 2.3 [2.0–2.6] (CS), BA bias 0.08 [−0.81–0.96], ICC 0.82; and E/e′ 4.6 [3.9–5.4] (conventional) vs. 3.8 [3.4–4.3] (CS), BA bias −0.90 [−2.31–0.50], ICC 0.89.
Data Conclusion: Analysis of intracardiac flow patterns and evaluation of diastolic function using a highly accelerated 4D flow sequence prototype is feasible, but it shows underestimation of flow measurements by approximately 10%.
Evidence Level: 2
Technical Efficacy: Stage 1

J. MAGN. RESON. IMAGING 2022.

Two-dimensional (2D) phase-contrast MRI has been an established clinical tool for vascular flow quantification; however, it is limited in the assessment of intracardiac flow due to the complexity of flow patterns and the changing geometry of the heart during the cardiac cycle.[1] The development of 4D flow techniques (i.e. time-resolved 3D imaging with

View this article online at wileyonlinelibrary.com. DOI: 10.1002/jmri.28484

Received Aug 2, 2022, Accepted for publication Oct 4, 2022.

*Address reprint requests to: T.E., Ashley River Tower, 25 Courtenay Drive, MSC 226, Charleston, South Carolina 29425-2260, USA.E-mail: emrich@musc.edu

From the [1]Division of Cardiovascular Imaging, Department of Radiology and Radiological Science, Medical University of South Carolina, Charleston, South Carolina; [2]Department of Diagnostic and Interventional Radiology, University Medical Center of the Johannes Gutenberg-University, Mainz, Germany; [3]German Centre for Cardiovascular Research, Partner site Rhine-Main, Mainz, Germany; [4]Siemens Medical Solutions USA Inc., Chicago, Illinois, USA; [5]Department of Radiology, Northwestern University, Feinberg School of Medicine, Chicago, Illinois, USA; and [6]Department of Biomedical Engineering, McCormick School of Engineering, Northwestern University, Evanston, Illinois, USA

Additional supporting information may be found in the online version of this article

three-directional velocity encoding) has not only addressed such limitations but also demonstrated high test–retest repeatability[2] and provided additional features, such as the option to retrospectively choose analysis locations within the acquired dataset or measure the ratio of pulmonary and systemic flows (Qp/Qs) within the same dataset.[3–6] The assessment of intracardiac flow parameters using the 4D flow technique has been demonstrated to have high reproducibility and consistency relative to 2D flow measurements.[7] Consensus statement guidelines have been released to facilitate the better understanding of 4D flow imaging and analysis techniques and to define potential clinical applications.[8,9] However, the widespread use of 4D flow remains limited due to the time-consuming nature of the acquisition.

Recent hardware and pulse sequence developments have resulted in improved time efficiency of 4D flow acquisitions. The compressed-sensing (CS) technique has been developed to accelerate MR data acquisition by combining incoherent acquisition and iterative reconstruction and has been successfully applied in 4D flow imaging. CS acceleration combined with respiratory controlled adaptive *k*-space reordering and inline image reconstruction has been shown to be feasible for highly accelerated aortic 4D flow acquisition with substantially reduced scan time (CS acceleration factor up to 14).[10] A similar CS 4D flow technique has been shown to provide comparable aortic flow measurements to those acquired using 4D flow with conventional parallel imaging, up to a CS acceleration factor of 6.[11] Beyond such acceleration, CS 4D flow may underestimate aortic flow parameters when compared to the reference conventional technique, as demonstrated in healthy volunteers.[10,11] While these studies show that the use of CS acceleration for 4D flow seems to be promising for relatively simple aortic applications, its application to more challenging intracardiac blood flow needs further exploration. Our hypothesis was that CS accelerated 4D flow MRI would allow for accurate intracardiac flow assessment.

Thus, the aim of this study was to compare intracardiac flow measurements between conventional and CS-based highly accelerated 4D flow acquisitions in healthy subjects.

Materials and Methods

Study Population

The study protocol was approved by the local institutional review board and written informed consent was obtained from all participants. Healthy volunteers were prospectively recruited with the following inclusion criteria: 1) >18 years of age and 2) no history of any cardiovascular disease. Subjects with MRI contraindications were excluded from the study.

MRI Acquisition

Volunteers underwent MR scans on a 3 T system (MAGNETOM Prisma, Siemens Healthcare, Erlangen, Germany). Prototype 4D flow acquisitions were performed 20 minutes postgadolinium contrast (0.1 mmol/kg gadobutrol; Gadavist, Bayer Healthcare, Berlin, Germany) as part of a comprehensive cardiac MRI protocol. Subjects were scanned in a head-first supine position using 32-element spine and 18-element surface phased-array coils. All acquisitions were retrospectively electrocardiographically (ECG) gated. Based on initial scout images, 2D balanced steady-state free precession (bSSFP) cine images were acquired to visualize the anatomy and motion of each cardiac valve in two orthogonal planes using the following typical pulse sequence parameters: acquired spatial resolution 1.7 × 1.3 × 6.0 mm^3; field of view (FoV) 340 mm × 340 mm; number of reconstructed cardiac time frames 25; echo time (TE)/repetition time (TR) 1.4/3.8 msec; temporal resolution 34 msec; and flip angle 52°.

Next, 4D flow acquisitions were planned in a sagittal orientation to cover the entire heart and the thoracic aorta. Image collection was performed during free-breathing under respiratory navigator gating and retrospective ECG-gating to evaluate the whole cardiac cycle. The respiratory navigator was positioned at the top of the right dome of the diaphragm and a 7 mm acceptance window was used. Conventional GeneRalized Autocalibrating Partial Parallel Acquisition (GRAPPA)[12] and CS accelerated 4D flow acquisitions were performed in random order and the acquisition durations noted. The CS 4D flow prototype pulse sequence was used for image acquisition.[10] CS 4D flow was undersampled using a spiral phyllotaxis subsampling pattern and reconstructed iteratively using spatio-temporal L1 regularization. Image reconstruction was fully integrated on the standard clinical scanner equipped with two graphical processing units (Tesla K10; NVIDIA, Santa Clara, CA, USA). Conventional and CS 4D flow acquisitions were performed in the same position and orientation using the typical pulse sequence parameters provided in Table 1.

Image Analysis

Postprocessing was performed by two readers (MH with 3 and TE with 12 years of experience in cardiac imaging) using a dedicated application for 4D flow analysis (CAAS MR Solutions v5.1, Pie Medical Imaging, Maastricht, The Netherlands). The presence of artifacts was evaluated by a reader (MH) to ensure that the overall image quality is sufficient for analysis. Each of the readers performed bSSFP cine assessment for left (LV) and right ventricular (RV) volumes and function, as well as conventional and CS 4D flow analyses independently, blinded to each other's results. The readers first evaluated all conventional image sets in random order. After a hiatus of at least 14 days to minimize recall bias, the readers assessed the CS 4D flow datasets in random order. Results reported represent the average of measurements obtained by the two readers. For intra-reader assessment, one of the readers reevaluated 10 random cases after a hiatus of 14 days.

bSSFP cine analysis was performed by semi-automatically segmenting the LV and RV blood pool and LV myocardium. End-diastolic volume (EDV, mL), end-systolic volume (ESV, mL), and stroke volume (SV = EDV-ESV, mL), as well as LV myocardial mass (g) were derived, and ejection fraction (EF = (SV/EDV) × 100, %) and cardiac output (SV × heart rate, liter/minute) were calculated.

Semi-automated valve tracking in the orthogonal views was performed for each valve using the bSSFP cine images, followed by manual delineation of the valve contours using the trans-valvular velocity maps as previously described.[13] Corrections for aliasing, static tissue offset, and valve motion were applied using built-in algorithms.[13] For each of the four valves, forward volume (mL), backward volume (mL), net forward volume (NFV; the difference between forward and backward volume, mL), and the regurgitation

TABLE 1. Typical Conventional and CS 4D Flow Pulse Sequence Parameters

	Conventional	CS
Acquired spatial resolution (mm)^3	2.4 × 3.5 × 3.8	2.4 × 3.5 × 3.6
Acquired matrix size	160 × 80 × 20	160 × 102 × 18
Reconstructed cardiac time frames	20	18–20
Echo time (msec)	2.28	2.36
Repetition time (msec)	4.83	5.06
Temporal resolution (msec)	38.64	40.48
Flip angle (°)	15	15
Pixel bandwidth (Hz/pixel)	495	460
VENC (cm/sec)	150	150
Acceleration factor	3[a]	7.7[b]

[a]GRAPPA = GeneRalized Autocalibrating Partial Parallel Acquisition.
[b]CS = compressed sensing.

fraction (%) were determined. In addition, cardiac output, Qp/Qs ratio (based on flow measured in the main pulmonary artery and the aorta), and parameters related to LV diastolic function, such as the ratio of early diastolic to late diastolic LV peak velocities (E/A ratio), and the ratio of early mitral inflow velocity to mitral annular early diastolic velocity (E/e′), were also determined. The percentage error (%error) of the CS 4D flow measurements relative to the conventional 4D flow assessment was calculated as follows:

$$\delta\,(\%) = \left|\frac{v_{\mathrm{CS}} - v_{\mathrm{Conventional}}}{v_{\mathrm{Conventional}}}\right| \times 100$$

where v_{CS} represents any given parameter measured by the CS 4D flow technique and $v_{\mathrm{Conventional}}$ represents the corresponding parameter obtained by the conventional 4D flow technique. Percentage error was also calculated for inter-reader differences.

In order to provide an internal reference and represent consistency, the NFV was measured and compared over all four valves as previously described.[13] The difference in NFV (ΔNFV) among the valves was calculated for each given valve as follows:

$$\Delta\mathrm{NFV}_i\,(\mathrm{mL}) = \mathrm{NFV}_i - \mathrm{mean}\left(\mathrm{NFV}_j\right), j \neq i, j = 1-4, i = 1-4$$

where NFV_i is the NFV and at any given valve and $\mathrm{mean}\left(\mathrm{NFV}_j\right)$ is the mean NFV across the other three valves.

Then, the variation in NFV among all four valves was expressed using the following formula:

$$\mathrm{NFV\ variation}\,(\%) = \frac{\sigma_{\Delta\mathrm{NFV}_i}}{\mathrm{mean\,NFV}_i} \times 100, i = 1-4$$

where $\sigma_{\Delta\mathrm{NFV}_i}$ is the standard deviation of ΔNFV over all four valves and $\mathrm{mean}(\mathrm{NFV}_i)$ is the mean of NFVs across all four valves.

Statistical Analysis

Statistical analysis was performed on SPSS v25 (IBM Corporation, Armonk, NY, USA) and plots were created in MedCalc 19.4 (MedCalc, Ostend, Belgium). The Kolmogorov–Smirnov test was used to assess the normality of continuous data. Continuous variables with normal distribution are reported as means ± standard deviations (SD), those with non-normal distribution are reported as median with interquartile range, and categoric variables as absolute frequencies and proportions. 4D flow measurements obtained by the conventional and CS techniques were compared using paired-samples *t*-test or Wilcoxon rank sum test, depending on distribution. Differences between the techniques were demonstrated using Bland–Altman plots by reporting the mean of differences and the 1.96 SD limits of agreement. Two-way mixed effects, absolute agreement and single rater intraclass correlations (ICC) were used to assess agreement between the various volumetric measurements at each valve obtained by the conventional vs. CS 4D flow techniques. ICC was also used to assess inter-reader and intra-reader agreement and was interpreted as follows: 0.0–0.3, lack of agreement; 0.31–0.5, weak agreement; 0.51–0.7, moderate agreement; 0.71–0.9, strong agreement; and 0.91–1.00, very strong agreement.[14] Minimal detectable change (MDC) was calculated to report the smallest change that occurs due to error and not likely related to chance variation in measurement.[15] Pearson's correlation was used to evaluate the correlation between measurements obtained by the different techniques and reported as Pearson's *r* coefficient. A *P*-value < 0.05 was considered significant.

Results

Our study cohort consisted of 50 healthy volunteers (mean age 28.0 ± 7.1 years, age range 20–58 years, 24 males [48%]). Volunteer characteristics derived from cardiac cine images are shown in Table 2.

TABLE 2. –Volunteer Characteristics; Cardiac Volumes and Function Data are Derived From Cine Images and Displayed as Mean and Standard Deviation or Median With [Interquartile Range] Depending on Data Distribution

Age (years)	**28.0 ± 7.1**
Gender (male)	24/50 (48%)
BMI (kg/m^2)	23.0 ± 2.7
BSA (m^2)	1.9 ± 0.2
LV EDV (mL)	160.5 ± 33.4
LV ESV (mL)	63.7 ± 17.4
LV SV (mL)	96.8 ± 19.6
LV EF (%)	60.6 ± 5.1
LV MASS (g)	99.1 ± 27.4
LV cardiac output (liter/minute)	6.8 [5.9–8.0]
RV EDV (mL)	160.7 [145.0–213.1]
RV ESV (mL)	76.0 [68.1–105.5]
RV SV (mL)	92.1 ± 25.5
RV EF (%)	51.5 [49.6–56.1]
RV cardiac output (l/min)	6.3 [5.5–7.7]

BMI = body mass index; BSA = body surface area; LV = left ventricle; EDV = end diastolic volume; ESV = end systolic volume; SV = stroke volume; EF = ejection fraction; RV = right ventricle.

The average acquisition time for conventional and CS 4D flow were 12.0 ± 1.3 and 6.7 ± 1.3 minutes, respectively, demonstrating a significant efficiency improvement by an average of 44%. All conventional and CS accelerated 4D flow studies provided sufficient image quality for intracardiac flow assessment. Representative images demonstrating 4D flow visualization at each cardiac valve are shown in Fig. 1 and Supplementary Video S1.

Flow measurements at the aortic, mitral, pulmonary, and tricuspid valves including forward volume, backward volume, NFV and regurgitation fraction are shown in Table 3 and Fig. 2. Representative flow curves of CS and conventional 4D flow over all four valves are shown in Fig. 3. Overall, a 3.3%–9.5% underestimation (% error in Table 3) was observed in large volumetric parameters (forward volume and NFV) measured by the CS technique relative to the conventional approach, the differences reaching statistical significance for almost every parameter. The underestimation was greater (6.6%–36.0%) for small volumetric measurements (backward volume). While there was strong agreement in the assessment of diastolic parameters (ICCs ≥ 0.82), there was a significant difference in mitral E/e′ assessment between the techniques (17.6% underestimation) (Table 3). The conventional and the CS techniques provided similar cardiac output for the LV (6.1 [5.5–7.0] liter/minute vs. 6.2 [5.6–7.0] liter/minute, respectively, $P = 0.739$), and for the RV (5.9 [5.4–7.2] liter/minute vs. 6.3 [5.6–7.1] liter/minute, respectively). A significant 4.3% underestimation of the LV and a nonsignificant 2.8% underestimation of the RV cardiac output ($P = 0.813$) were observed by the CS 4D flow technique compared to results obtained by the clinical reference standard bSSFP cine imaging (LV: 6.8 [5.9–8.0] liter/minute and RV: 6.3 [5.5–7.7] liter/minute).

Correlation analysis for forward volume and NFV between conventional and CS 4D flow showed strong agreement at all four valves (all $r > 0.81$; Table 3 and Fig. 4). Correlation was moderate, but significant for all other parameters (all $r > 0.34$). ICCs (Table 3) demonstrated strong to very

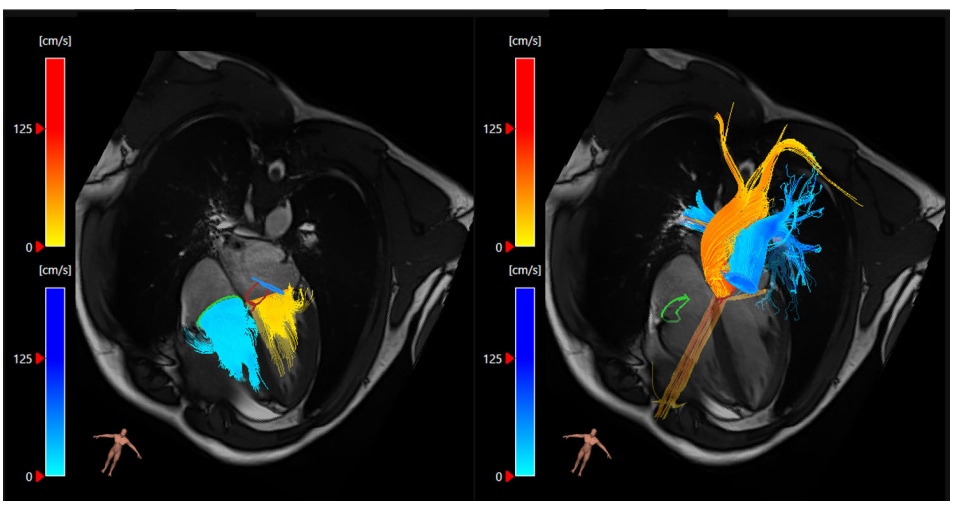

FIGURE 1: Representative images showing tricuspid and mitral flow (left) and aortic and pulmonary flow (right) visualization in a healthy volunteer.

TABLE 3. 4D Flow-Derived Intracardiac Parameters Measured by the Conventional and the CS Accelerated Techniques

	Conventional	CS	*P*	ICC	*r*	%error
Heart rate (beats/min)	70 ± 10	77 ± 12	<0.001			
Qp/Qs	0.98 ± 0.06	1.02 ± 0.05	<0.001	0.62	0.59**	5.0
Aortic valve						
Forward volume (mL)	94.3 ± 16.7	86.6 ± 15.4	<0.001	0.97	0.94**	8.0
Backward volume (mL)	3.0 ± 1.4	2.6 ± 1.3	0.133	0.64	0.47**	25.4
Net forward volume (mL)	91.3 ± 16.5	83.9 ± 14.8	<0.001	0.96	0.92**	7.8
Regurgitation fraction (%)	3.1 ± 1.4	3.0 ± 1.4	0.679	0.58	0.41**	36.0
LV cardiac output (liter/minute)	6.1 [5.5–7.0]	6.2 [5.6–7.0]	0.739	0.92	0.88**	1.7
Mitral valve						
Forward volume (mL)	98.8 ± 19.1	93.0 ± 17.4	<0.001	0.92	0.85**	5.3
Backward volume (mL)	4.7 [3.3–5.6]	3.4 [2.7–4.2]	<0.001	0.70	0.54**	18.4
Net forward volume (mL)	94.0 ± 18.4	89.3 ± 17.2	0.002	0.91	0.84**	4.4
Regurgitation fraction (%)	5.0 [3.5–6.0]	4.0 [3.0–5.0]	0.004	0.60	0.43**	11.5
E/A	2.2 [1.9–2.4]	2.3 [2.0–2.6]	0.158	0.82	0.69**	3.2
E/e′	4.6 [3.9–5.4]	3.8 [3.4–4.3]	<0.001	0.89	0.83**	17.6
Pulmonary valve						
Forward volume (mL)	91.3 ± 15.7	87.9 ± 14.3	<0.001	0.96	0.92**	3.4
Backward volume (mL)	1.9 [1.2–3.1]	1.9 [1.1–3.0]	0.132	0.79	0.67**	6.6
Net forward volume (mL)	89.0 ± 14.8	85.7 ± 13.8	0.001	0.95	0.90**	3.3
Regurgitation fraction (%)	2.5 [1.5–3.0]	2.0 [1.5–3.0]	0.202	0.73	0.58**	6.6
RV cardiac output (liter/minute)	5.9 [5.4–7.2]	6.3 [5.6–7.1]	<0.001	0.89	0.85**	6.6
Tricuspid valve						
Forward volume (mL)	105.9 ± 18.5	95.5 ± 18.0	<0.001	0.83	0.83**	9.5
Backward volume (mL)	5.7 ± 2.9	4.0 ± 1.9	<0.001	0.60	0.47**	16.4
Net forward volume (mL)	100.2 ± 17.4	91.6 ± 17.1	<0.001	0.89	0.81**	8.3
Regurgitation fraction (%)	5.3 ± 2.5	4.1 ± 1.7	0.001	0.49	0.34*	6.4

Descriptive data are displayed as mean ± standard deviation or median with [IQR] depending on data distribution. Date reported are the average measurements of the two readers.
CS = compressed sensing; IQR = interquartile range; ICC = intraclass correlation coefficient; *r* = Pearson's correlation coefficient; LV = left ventricle; RV = right ventricle.
*Significant at the 0.05 level.
**Significant at the 0.01 level.

strong agreement between conventional and CS 4D flow for forward volume and NFV (all ICCs > 0.83). However, agreement in backward volume and regurgitation fraction was weak to strong between the techniques (ICCs in the range a 0.49–0.79). Diastolic function parameters, on the other hand, showed strong agreement with ICCs between 0.82–0.89 (Table 3). There was a significant difference in Qp/Qs ratios between the techniques, the mean difference being 0.05 with −0.06 and 0.15 as lower and upper limits of agreement (Fig. 5).

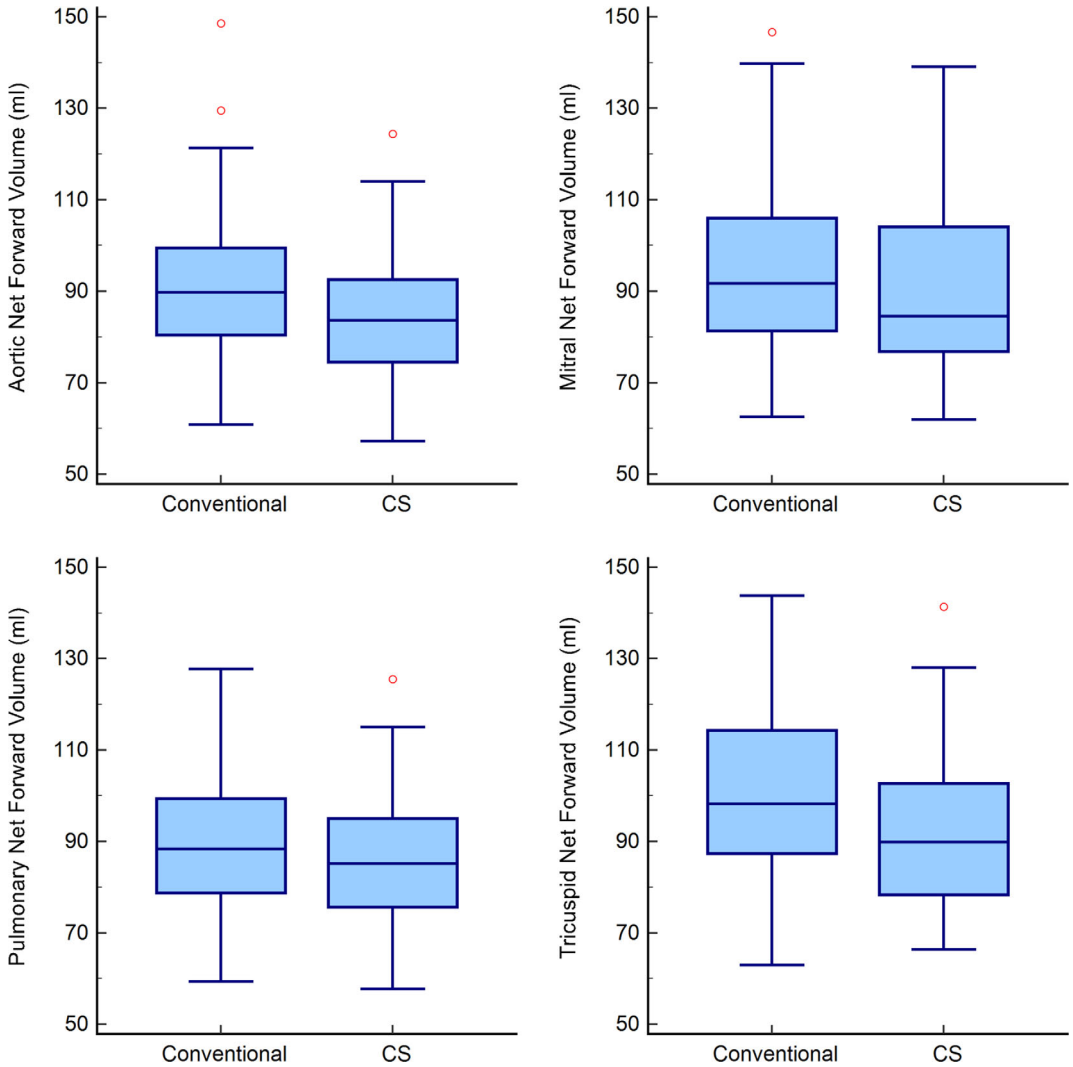

FIGURE 2: Comparison of the net forward volumes measured at all four cardiac valves by the conventional and CS 4D flow techniques represented by box plots.

Bland–Altman plots demonstrated similar underestimation of NFV for all four valves by the CS 4D flow technique compared to the conventional approach (Fig. 6). The mean of differences and [lower/upper limits of agreement] for the aortic, mitral, pulmonary, and tricuspid valve NFVs were −7.3 mL [−19.7; 5.1], −4.5 mL [−24.3; 15.3], −3.2 mL [−15.7; 9.2], and −8.7 mL [−29.6; 12.3], respectively.

For each technique, inter-reader variability calculated for the different flow parameters at each valve (Table 4) demonstrated very strong agreement (ICCs ranging between 0.94 and 0.99) except for measurements involving very small volumes such as <6 mL backward volumes and their derived parameters (ICCs ranging between 0.23 and 0.95). MDCs calculated between the readers are also reported in Table 4. The %error between the readers was low for large volumes across all valves for both conventional (forward volume 2.8% and NFV 3.2%) and CS (forward volume 2.3% and NFV 2.7%) techniques. However, larger inter-reader %error was found for backward volume (conventional 52.4% vs. CS 63.9%).

Intra-reader agreement was moderate to very strong with ICCs between 0.58 and 0.99 (Table 4), with no substantial difference between the techniques.

Differences and variations in NFV compared between the techniques over all four cardiac valves are reported in Table 5. Despite significant differences between the techniques, the mean variations remained under 10%.

Discussion

In this study, we demonstrated the feasibility of using CS accelerated 4D flow acquisition for the assessment of intracardiac flow parameters. Overall, our results indicate that intracardiac flow parameters can be obtained by CS 4D flow and measurements show significant correlation and strong to very strong agreement for forward volume and NFV with an underestimation of <10%, compared to those derived from conventional 4D flow acquisition. While significant correlation was also observed for backward volume, the agreement

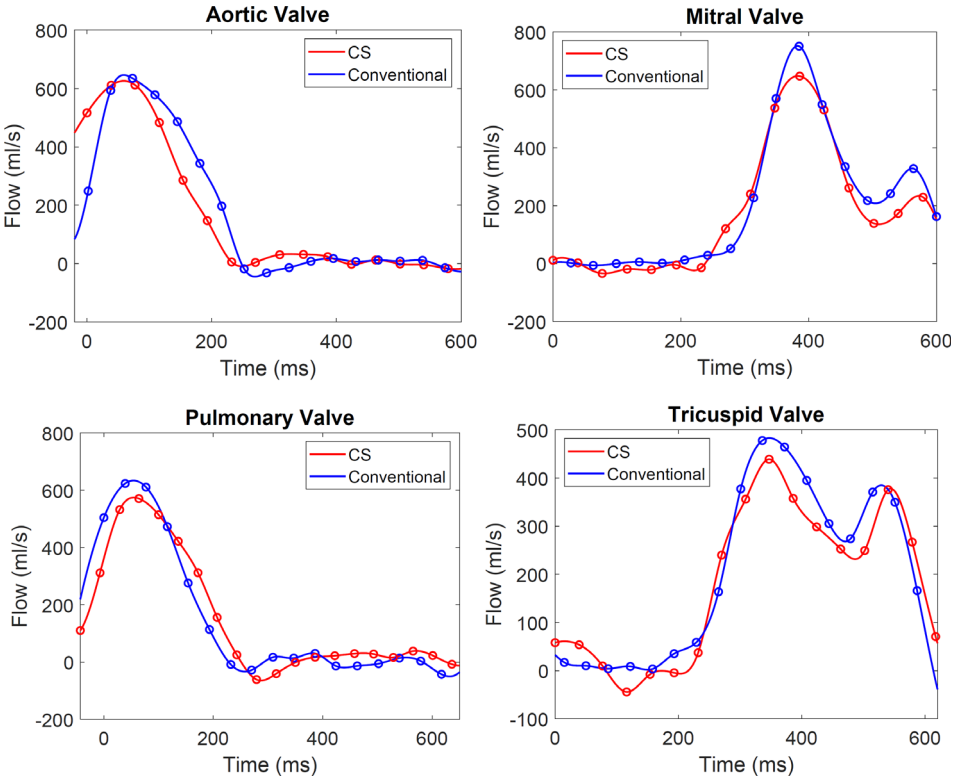

FIGURE 3: Typical flow curves from the same volunteer demonstrating underestimation of peak flow by CS 4D flow (red) in comparison to conventional 4D flow (blue) at all valves. The %error for peak flow was: aortic valve 3.1%, mitral valve 13.8%, pulmonary valve 9.3%, and tricuspid valve 9.1%.

between CS and conventional 4D flow measurements was moderate to strong with an average error of 17%.

We have demonstrated significant time efficiency improvement using the CS 4D flow technique. While there are trade-offs as discussed below, highly accelerated 4D flow seems to be able to address one of the major limitations to conventional 4D flow, that is, the time-consuming image acquisition, which is often difficult to fit into standard clinical protocols. Other factors, such as improved patient compliance especially in the pediatric population, can also be considered a potential benefit of shortened acquisition time.

While there were significant differences between the majority of the flow parameters obtained by the two techniques, these deviations were relatively small for large volumes (i.e. forward volume and NFV). Although, a clear underestimation by the CS technique can be seen on the Bland–Altman plots, such underestimation by CS accelerated 4D flow techniques has been experienced and described before in thoracic aorta studies,[11,16] and similar underestimation has also been demonstrated by the k-t BLAST highly accelerated technique in the aorta and the pulmonary arteries.[17] While using a CS acceleration factor of 6 provided accurate assessment of flow parameters using a different scanner platform,[11] the acceleration factor of 7.7 in this study was chosen to further improve the time efficiency of the acquisition while keeping measurement inaccuracy small and clinically irrelevant. The reason for the differences between conventional and CS-based 4D flow measurements may be attributed to the spatial and temporal smoothing effect caused by spatial and temporal regularization, and higher noise values arising from higher acceleration levels.[11]

In this study, we observed a strong correlation between parameters measured by the conventional and the CS 4D flow techniques. Such strong agreement was mostly seen for measuring large volume parameters; however, only weak-to-moderate agreement with high %error was demonstrated for the assessment of small volumes. Such differences potentially arose from the negligible volume of regurgitation in this healthy volunteer population, resulting in limited ability to draw regions of interest in the regurgitant area. The reported high intermodality and inter-reader %error explains the modest agreement in backward volume, however, it needs to be noted that such high %error corresponds to <3 mL volume difference. As demonstrated by Feneis et al, 4D flow assessment of mitral and tricuspid regurgitation shows high correlation with 2D flow evaluation in patients with substantial (29%–42%) regurgitant fraction; however, the Pearson's and ICC values were consistently lower for 4D flow compared to 2D flow.[7] Furthermore, we have demonstrated comparable results for both techniques for the quantification of cardiac output. In comparison with quantification by bSSFP cine imaging, both 4D flow techniques underestimated cardiac

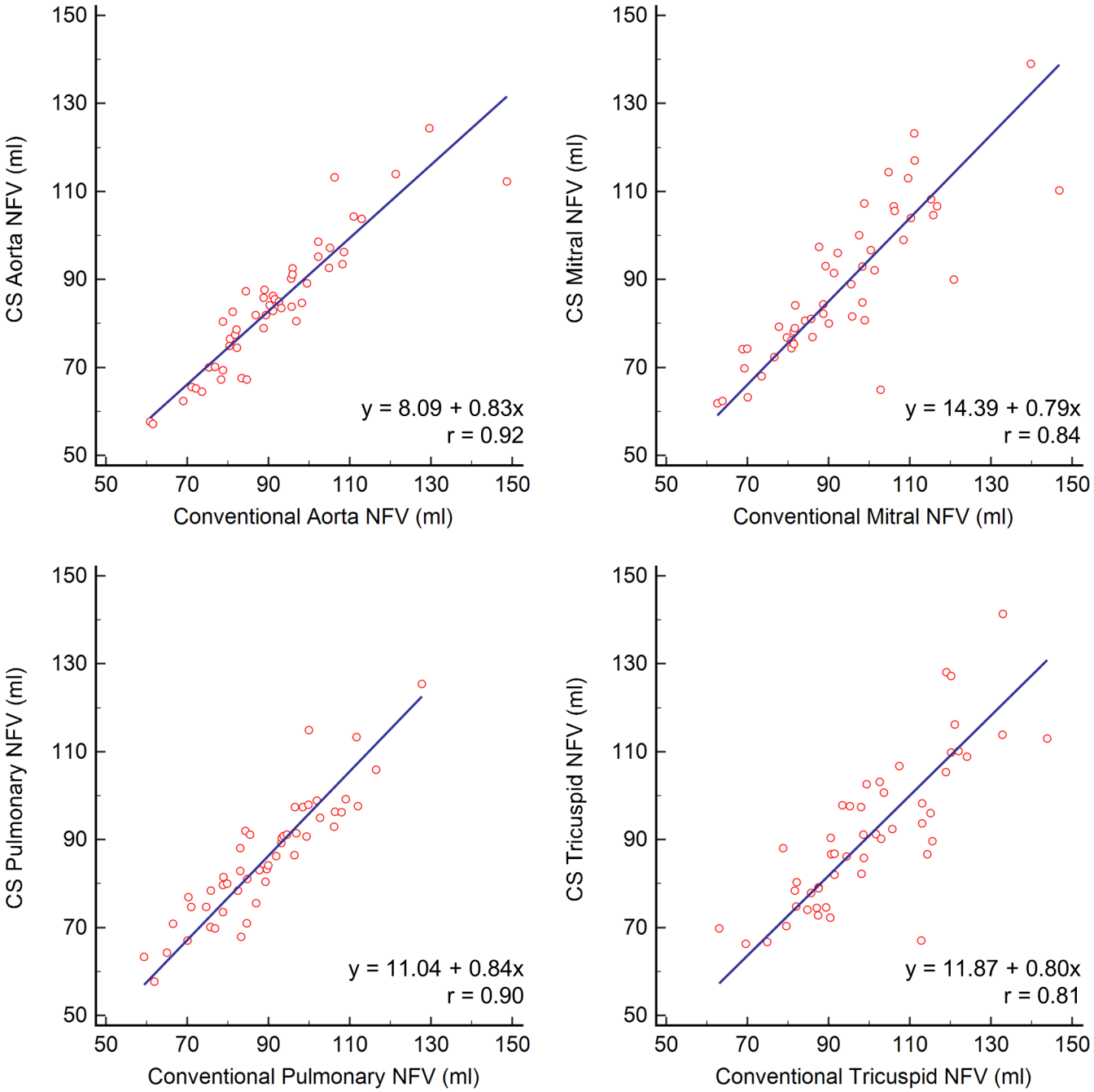

FIGURE 4: Scatter plots demonstrating correlation between net forward volumes (NFV) at different valves measured by the conventional and CS 4D flow techniques.

output. This result is similar to that shown in a recent animal study[18] where despite underestimation, the 4D flow-based cardiac output showed stronger correlation and lower divergence to simultaneous invasive flow measurements, compared with 2D flow. The evaluation of a commonly used phase-contrast imaging-based clinical parameter, the Qp/Qs-ratio, showed significant, but clinically irrelevant, differences between the two 4D flow techniques. Therefore, despite the slight, but systematic underestimation of flow parameters, our results indicate that calculation of flow ratios may be feasible using the CS 4D flow technique. In addition, internal consistency of the 4D flow measurements represented by NFV variation over all four valves was similar for conventional and CS 4D flow techniques, and in a range similar to that described for conventional techniques.[13] Therefore, the physiological principle of mass conservation over all four valves is retained in an acceptable range, even when image acceleration with CS is applied.

There have been a few acceleration techniques proposed for 4D flow acquisition. 3D phase-contrast vastly undersampled isotropic projection reconstruction (PC-VIPR) has been shown to provide good image quality even at high

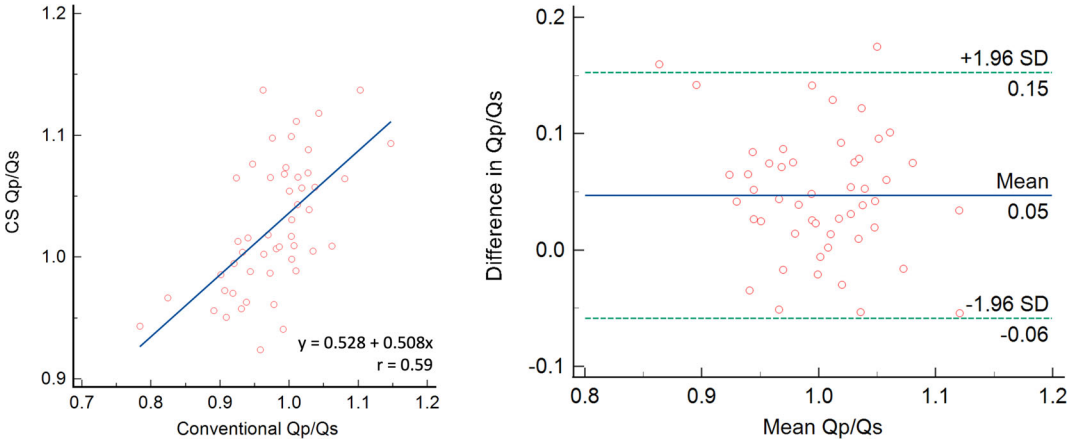

FIGURE 5: Scatter and Bland–Altman plots demonstrating the correlation and agreement between Qp/Qs derived by conventional and CS 4D flow techniques.

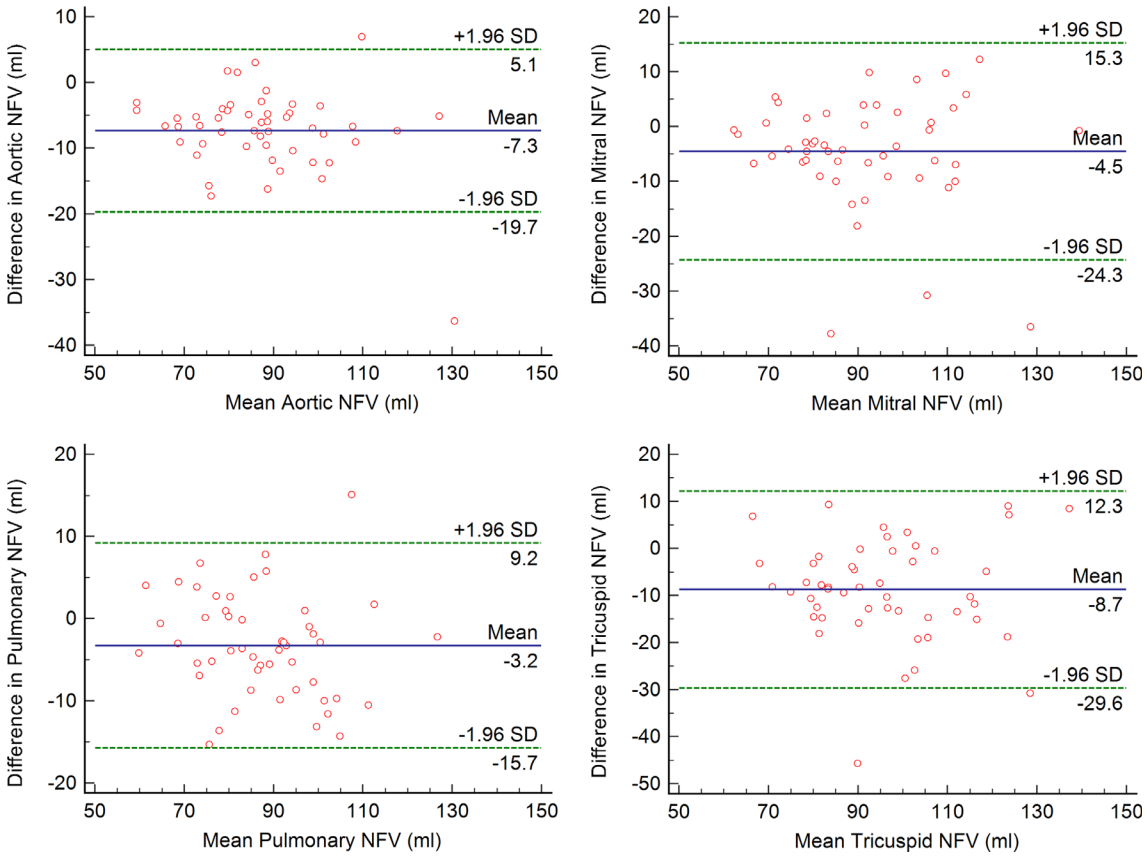

FIGURE 6: Bland–Altman plots representing the agreement in net forward volumes (NFV) between the conventional and CS-based 4D flow techniques. Blue solid lines show the mean of differences, while the green dotted lines indicate the upper and lower limits of agreement (±1.96 SD). A <9 mL underestimation in NFV by the CS technique was observed for each valve.

acceleration (with acceleration factors between 17 and 60); however, it underestimated flow parameters by 6%.[19] k-t principal component analysis[20] has been reported as an 8-fold accelerated 4D flow technique providing high correlation with 2D phase-contrast imaging, but demonstrating a similar underestimation (5%) of flow values in the great vessels.[21] A more recent study using k-t accelerated nongated 4D flow employing parallel MRI with extended and averaged (PEAK) GRAPPA (acceleration factor 5) has shown the feasibility of a 2-minute protocol, with moderate (5%–22%) underestimation of flow values.[22] The Bayes approach has also been validated in phantoms and volunteers for a single breath-hold aortic valve 4D flow acquisition and was found to be feasible at acceleration rates up to 27.[23] While all the acceleration techniques provide substantial improvement in scan efficiency, their effect on the accuracy of flow quantification

TABLE 4. Inter-reader ($n = 50$) and Intra-reader ($n = 10$) Agreement, As Well As Minimal Detectable Change Between the Readers for the Various Flow Parameters

	Inter-reader ICC		Intra-reader ICC		MDC	
	Conventional	CS	Conventional	CS	Conventional	CS
Qp/Qs	0.87	0.70	0.57	0.45	0.06	0.07
Aortic valve						
Forward volume	0.99	0.99	0.99	0.99	4.62	4.26
Backward volume	0.90	0.70	0.95	0.99	1.22	1.97
Net forward volume	0.99	0.99	0.99	0.99	4.57	4.10
Regurgitation fraction	0.85	0.70	0.91	0.97	1.50	2.12
LV Cardiac output	0.99	0.99	0.99	0.99	0.34	0.43
Mitral valve						
Forward volume	0.99	0.99	0.99	0.99	5.29	4.82
Backward volume	0.48	0.72	0.74	0.89	3.56	2.38
Net forward volume	0.98	0.98	0.99	0.99	7.21	6.74
Regurgitation fraction	0.31	0.65	0.78	0.91	0.03	0.02
E/A	0.95	0.92	0.92	0.98	0.34	0.50
E/e′	0.87	0.86	0.75	0.98	1.27	1.01
Pulmonary valve						
Forward volume	0.98	0.97	0.86	0.89	6.15	6.86
Backward volume	0.81	0.75	0.71	0.85	1.96	1.74
Net forward volume	0.98	0.97	0.87	0.90	5.80	6.62
Regurgitation fraction	0.75	0.72	0.70	0.85	0.02	0.02
RV Cardiac output	0.99	0.99	0.94	0.98	0.36	0.44
Tricuspid valve						
Forward volume	0.99	0.96	0.97	0.96	5.12	9.97
Backward volume	0.77	0.51	0.71	0.58	3.85	3.68
Net forward volume	0.98	0.94	0.95	0.95	6.82	11.61
Regurgitation fraction	0.73	0.23	0.73	0.67	3.60	4.13

CS = compressed sensing; ICC = intraclass correlation coefficient; MDC = minimal detectable change; LV = left ventricle; RV = right ventricle.

needs to be carefully considered, especially when imaging children with smaller flow volumes.

Implementation of CS in 4D flow acquisitions has been reported for vascular and qualitative intracardiac applications. The accuracy and precision of parallel imaging CS 4D flow-based quantification of venous flow have been reported comparable to arterial flow in patients with shunts.[24] The combination of spiral sampling and dynamic CS has been used for 4D flow imaging of the abdominal vessels with results showing underestimation of flow parameters compared to Cartesian 4D flow imaging.[25] Similar underestimation has been reported by Cheng et al using multidimensional XD flow imaging that enables respiratory and cardiac motion resolved reconstruction.[26] Finally, a variable density Poisson-disk sampling pattern-based CS 4D flow technique has been shown to improve the sensitivity of detection of hemodynamically significant shunts and valvular insufficiency, compared to conventional cardiac MRI.[27]

TABLE 5. Difference and Variation in Net Forward Volume Across All Valves

	Conventional	CS	*P*
ΔNFV aortic valve (mL)	−4.6 ± 4.9	−4.8 ± 6.5	0.757
ΔNFV mitral valve (mL)	0.3 ± 5.2	2.2 ± 7.4	0.100
ΔNFV pulmonary valve (mL)	−6.1 ± 5.7	−2.5 ± 7.0	0.001
ΔNFV tricuspid valve (mL)	5.1 ± 4.5	5.2 ± 7.9	0.947
NFV variation (%)	5.5 ± 0.8	8.9 ± 0.4	0.011

CS = compressed sensing; NFV = net forward volume; ΔNFV = NFV difference.

However, quantitative intracardiac flow evaluation was not performed in the latter work.

As demonstrated in the studies above, highly accelerated 4D flow techniques tend to underestimate flow measures, similarly as reported in this study. Such underestimation may be caused by temporal undersampling generally characteristic for high acceleration.[10] CS reconstruction with increasing regularization can cause temporal blurring of flow data that may lead to the observed underestimation. As a remedy, the additional temporal incoherence introduced by iterative Golden-angle RAdial Sparse Parallel (iGRASP) MRI[28] or the perturbed spiral real-time phase-contrast MRI[29] can help to reduce such effects. Other different reconstruction or regularization approaches, for example, the Reconstructing Velocity Encoded MRI with Approximate message passing aLgorithms (ReVEAL),[30] can be investigated to improve the measurement accuracy of peak velocities.

Despite such underestimation, highly accelerated CS techniques deliver important benefits as has been demonstrated in cine,[31] perfusion,[32] and MR angiography.[33] CS acceleration increases the speed of image acquisition, improves efficiency and consequently patient compliance, and allows for imaging patients with limited breath-hold capacity. The increased availability of CS techniques may improve scanner utilization due to shorter scan time, resulting in lower cost and higher patient throughput. While the timeline when CS techniques will be generally available is unclear, our investigation contributes to the constantly growing literature establishing their clinical applications.

Limitations

While we believe that the size of the study cohort was adequate for feasibility evaluation, the inclusion of only a young healthy volunteer population with low BMI limits the extrapolation of our results to a real-world clinical scenario. As demonstrated, the measurement of small regurgitant volumes shows limited interobserver agreement and accuracy; thus, the evaluation of patients with quantifiable regurgitation is necessary to establish the value of CS 4D flow for intracardiac applications. Additionally, the assessment of complex intracardiac flow patterns in patients with shunts and congenital heart diseases also needs further investigation. The 4D flow protocol used in this study included data acquisition of the heart and the aorta, which required the use of a relatively high (150 cm/sec) VENC, resulting in potentially increased noise. Furthermore, there was an unexpected significant difference in heart rate between the two 4D flow acquisitions, which may have influenced the measured flow parameters. Finally, this study did not evaluate the effect of gadolinium contrast administration on the accuracy of the flow parameters compared to native scans; however, flow acquisitions are often performed postcontrast at the end of the MRI protocol and therefore benefit from increased signal-to-noise and velocity-to-noise ratios.[34,35]

Conclusion

This study demonstrated the feasibility of analyzing intracardiac flow patterns and evaluating diastolic function using a highly accelerated CS 4D flow sequence prototype, with good agreement to measurements obtained by conventional 4D flow imaging.

Acknowledgments

The authors want to thank Petra Rieck, Kristin Berg and Lydia Vehling for their technical support of our study. In addition, they thank Gaston Vogel from Pie Medical Imaging, Maastricht, the Netherlands, for providing the CAAS MR Solutions v5.1 software and software training. The manuscript contains data from the doctoral theses of two authors (A.K. and A.E.). Open Access funding enabled and organized by Projekt DEAL.

Conflict of interest

U. Joseph Schoepf receives institutional research support and/or personal fees from Bayer, Bracco, Elucid Bioimaging, Guerbet, HeartFlow, and Siemens. Akos Varga-Szemes receives institutional research support and/or personal fees from Bayer, Elucid Bioimaging and Siemens. Tilman Emrich

received a speaker fee and travel support from Siemens Medical Solutions USA Inc. Ning Jin and Fei Xiong are employees of Siemens Medical Solutions USA Inc. Michael Markl receives research support from Siemens Healthineers, has research grants from Circle Cardiovascular Imaging and Cryolife Inc, and receives consulting fees from Circle Cardiovascular Imaging. The other authors have no conflict of interest to disclose.

References

1. Rodriguez Munoz D, Markl M, Moya Mur JL, et al. Intracardiac flow visualization: Current status and future directions. Eur Heart J Cardiovasc Imaging 2013;14(11):1029-1038.
2. Stoll VM, Loudon M, Eriksson J, et al. Test-retest variability of left ventricular 4D flow cardiovascular magnetic resonance measurements in healthy subjects. J Cardiovasc Magn Reson 2018;20(1):15.
3. van der Geest RJ, Garg P. Advanced analysis techniques for intracardiac flow evaluation from 4D flow MRI. Curr Radiol Rep 2016;4:38.
4. Crandon S, Elbaz MSM, Westenberg JJM, van der Geest RJ, Plein S, Garg P. Clinical applications of intra-cardiac four-dimensional flow cardiovascular magnetic resonance: A systematic review. Int J Cardiol 2017;249:486-493.
5. Markl M, Schnell S, Wu C, et al. Advanced flow MRI: Emerging techniques and applications. Clin Radiol 2016;71(8):779-795.
6. Hanneman K, Sivagnanam M, Nguyen ET, et al. Magnetic resonance assessment of pulmonary (QP) to systemic (QS) flows using 4D phase-contrast imaging: Pilot study comparison with standard through-plane 2D phase-contrast imaging. Acad Radiol 2014;21(8):1002-1008.
7. Feneis JF, Kyubwa E, Atianzar K, et al. 4D flow MRI quantification of mitral and tricuspid regurgitation: Reproducibility and consistency relative to conventional MRI. J Magn Reson Imaging 2018;48(4):1147-1158.
8. Dyverfeldt P, Bissell M, Barker AJ, et al. 4D flow cardiovascular magnetic resonance consensus statement. J Cardiovasc Magn Reson 2015;17:72.
9. Zhong L, Schrauben EM, Garcia J, et al. Intracardiac 4D flow MRI in congenital heart disease: Recommendations on behalf of the ISMRM flow & motion study group. J Magn Reson Imaging 2019;50(3):677-681.
10. Ma LE, Markl M, Chow K, et al. Aortic 4D flow MRI in 2 minutes using compressed sensing, respiratory controlled adaptive k-space reordering, and inline reconstruction. Magn Reson Med 2019;81(6):3675-3690.
11. Neuhaus E, Weiss K, Bastkowski R, Koopmann J, Maintz D, Giese D. Accelerated aortic 4D flow cardiovascular magnetic resonance using compressed sensing: Applicability, validation and clinical integration. J Cardiovasc Magn Reson 2019;21(1):65.
12. Griswold MA, Jakob PM, Heidemann RM, et al. Generalized autocalibrating partially parallel acquisitions (GRAPPA). Magn Reson Med 2002;47(6):1202-1210.
13. Kamphuis VP, Roest AAW, Ajmone Marsan N, et al. Automated cardiac valve tracking for flow quantification with four-dimensional flow MRI. Radiology 2019;290(1):70-78.
14. Emrich T, Bordonaro V, Schoepf UJ, et al. Right/left ventricular blood Pool T2 ratio as an innovative cardiac MRI screening tool for the identification of left-to-right shunts in patients with right ventricular disease. J Magn Reson Imaging 2022;55(5):1452-1458.
15. Muckelt PE, Warner MB, Cheliotis-James T, et al. Protocol and reference values for minimal detectable change of MyotonPRO and ultrasound imaging measurements of muscle and subcutaneous tissue. Sci Rep 2022;12(1):13654.
16. Pathrose A, Ma L, Berhane H, et al. Highly accelerated aortic 4D flow MRI using compressed sensing: Performance at different acceleration factors in patients with aortic disease. Magn Reson Med 2021;85(4):2174-2187.
17. Carlsson M, Toger J, Kanski M, et al. Quantification and visualization of cardiovascular 4D velocity mapping accelerated with parallel imaging or k-t BLAST: Head to head comparison and validation at 1.5 T and 3 T. J Cardiovasc Magn Reson 2011;13:55.
18. Stam K, Chelu RG, van der Velde N, et al. Validation of 4D flow CMR against simultaneous invasive hemodynamic measurements: A swine study. Int J Cardiovasc Imaging 2019;35(6):1111-1118.
19. Gu T, Korosec FR, Block WF, et al. PC VIPR: A high-speed 3D phase-contrast method for flow quantification and high-resolution angiography. AJNR Am J Neuroradiol 2005;26(4):743-749.
20. Giese D, Schaeffter T, Kozerke S. Highly undersampled phase-contrast flow measurements using compartment-based k-t principal component analysis. Magn Reson Med 2013;69(2):434-443.
21. Giese D, Wong J, Greil GF, Buehrer M, Schaeffter T, Kozerke S. Towards highly accelerated Cartesian time-resolved 3D flow cardiovascular magnetic resonance in the clinical setting. J Cardiovasc Magn Reson 2014;16:42.
22. Bollache E, Barker AJ, Dolan RS, et al. k-t accelerated aortic 4D flow MRI in under two minutes: Feasibility and impact of resolution, k-space sampling patterns, and respiratory navigator gating on hemodynamic measurements. Magn Reson Med 2018;79(1):195-207.
23. Rich A, Potter LC, Jin N, Liu Y, Simonetti OP, Ahmad R. A Bayesian approach for 4D flow imaging of aortic valve in a single breath-hold. Magn Reson Med 2019;81(2):811-824.
24. Tariq U, Hsiao A, Alley M, Zhang T, Lustig M, Vasanawala SS. Venous and arterial flow quantification are equally accurate and precise with parallel imaging compressed sensing 4D phase contrast MRI. J Magn Reson Imaging 2013;37(6):1419-1426.
25. Dyvorne H, Knight-Greenfield A, Jajamovich G, et al. Abdominal 4D flow MR imaging in a breath hold: Combination of spiral sampling and dynamic compressed sensing for highly accelerated acquisition. Radiology 2015;275(1):245-254.
26. Cheng JY, Zhang T, Alley MT, et al. Comprehensive multi-dimensional MRI for the simultaneous assessment of cardiopulmonary anatomy and physiology. Sci Rep 2017;7(1):5330.
27. Hsiao A, Lustig M, Alley MT, Murphy MJ, Vasanawala SS. Evaluation of valvular insufficiency and shunts with parallel-imaging compressed-sensing 4D phase-contrast MR imaging with stereoscopic 3D velocity-fusion volume-rendered visualization. Radiology 2012;265(1):87-95.
28. Feng L, Grimm R, Block KT, et al. Golden-angle radial sparse parallel MRI: Combination of compressed sensing, parallel imaging, and golden-angle radial sampling for fast and flexible dynamic volumetric MRI. Magn Reson Med 2014;72(3):707-717.
29. Kowalik GT, Knight D, Steeden JA, Muthurangu V. Perturbed spiral real-time phase-contrast MR with compressive sensing reconstruction for assessment of flow in children. Magn Reson Med 2020;83(6):2077-2091.
30. Pruitt A, Rich A, Liu Y, et al. Fully self-gated whole-heart 4D flow imaging from a 5-minute scan. Magn Reson Med 2021;85(3):1222-1236.
31. Vermersch M, Longere B, Coisne A, et al. Compressed sensing real-time cine imaging for assessment of ventricular function, volumes and mass in clinical practice. Eur Radiol 2020;30(1):609-619.
32. Hong K, Collins JD, Freed BH, et al. Accelerated wideband myocardial perfusion pulse sequence with compressed sensing reconstruction for myocardial blood flow quantification in patients with a cardiac implantable electronic device. Radiol Cardiothorac Imaging 2020;2(2):e190114.
33. Zhu C, Cao L, Wen Z, et al. Surveillance of abdominal aortic aneurysm using accelerated 3D non-contrast black-blood cardiovascular magnetic resonance with compressed sensing (CS-DANTE-SPACE). J Cardiovasc Magn Reson 2019;21(1):66.
34. Bock J, Frydrychowicz A, Stalder AF, et al. 4D phase contrast MRI at 3 T: Effect of standard and blood-pool contrast agents on SNR, PC-MRA, and blood flow visualization. Magn Reson Med 2010;63(2):330-338.
35. Hess AT, Bissell MM, Ntusi NA, et al. Aortic 4D flow: Quantification of signal-to-noise ratio as a function of field strength and contrast enhancement for 1.5T, 3T, and 7T. Magn Reson Med 2015;73(5):1864-1871.